environmental microbiology

Environmental Microbiology (2021) **23**(8), 4228–4245 doi:10.1111/1462-2920.15600

Characterization and phylogenomic analysis of *Breznakiella homolactica* gen. nov. sp. nov. indicate that termite gut treponemes evolved from non-acetogenic spirochetes in cockroaches

Yulin Song,[1] **Vincent Hervé**,[1] **Renate Radek**,[2] **Fabienne Pfeiffer**,[1] **Hao Zheng**[1] **and Andreas Brune**[1*]

[1]*Research Group Insect Gut Microbiology and Symbiosis, Max Planck Institute for Terrestrial Microbiology, Karl-von-Frisch-Str. 10, Marburg, 35043, Germany.*

[2]*Institute of Biology/Zoology, Free University of Berlin, Königin-Luise-Str. 1-3, Berlin, 14195, Germany.*

Summary

Spirochetes of the genus *Treponema* are surprisingly abundant in termite guts, where they play an important role in reductive acetogenesis. Although they occur in all termites investigated, their evolutionary origin is obscure. Here, we isolated the first representative of 'termite gut treponemes' from cockroaches, the closest relatives of termites. Phylogenomic analysis revealed that *Breznakiella homolactica* gen. nov. sp. nov. represents the most basal lineage of the highly diverse 'termite cluster I', a deep-branching sister group of *Treponemataceae* (fam. '*Termitinemataceae*') that was present already in the cockroach ancestor of termites and subsequently coevolved with its host. *Breznakiella homolactica* is obligately anaerobic and catalyses the homolactic fermentation of both hexoses and pentoses. Resting cells produced acetate in the presence of oxygen. Genome analysis revealed the presence of pyruvate oxidase and catalase, and a cryptic potential for the formation of acetate, ethanol, formate, CO_2 and H_2 - the fermentation products of termite gut isolates. Genes encoding key enzymes of reductive acetogenesis, however, are absent, confirming the hypothesis that the ancestral metabolism of the cluster was fermentative, and that the capacity for acetogenesis from H_2 plus CO_2 - the most intriguing property among termite gut treponemes - was acquired by lateral gene transfer.

Introduction

Spirochetes (phylum *Spirochaetes*) are morphologically distinct bacteria with highly motile, helical cells composed of a protoplasmic cylinder and periplasmic flagella that are enclosed in an outer sheath (Paster, 2015). They are widespread in a variety of environments but typically occur only in low numbers. A notable exception is the hindgut of termites, where spirochetes predominate the bacterial microbiota, particularly in the wood-feeding taxa (Brune, 2014; Mikaelyan *et al*., 2015a). Here, they occur either free-living or associated with cellulolytic protists and can make up more than one-half of the bacterial population (Breznak, 2002; Breznak and Leadbetter, 2006; Ohkuma and Brune, 2011).

The high abundance of spirochetes in the hindgut of termites was first described by Joseph Leidy ('*Vibrio termitis*'; Leidy, 1881) and has puzzled biologists ever since. For a long time, termite gut spirochetes remained uncultured and (if at all) were classified only on a morphological basis; none of these names has been validly published (Breznak, 2002; Paster, 2018). However, with the advent of 16S rRNA-gene-based phylogenies, it became clear that almost all termite gut spirochetes fall into the radiation of the genus *Treponema*, where they form two distinct clades (Berchtold *et al*., 1994; Ohkuma and Kudo, 1996; Paster *et al*., 1996). The larger of the two clades, referred to as 'termite cluster' (Lilburn *et al*., 1999) or 'termite *Treponema* cluster I' (Ohkuma *et al*., 1999), hereafter 'termite cluster I', is extremely diverse and seems to occur in all termite species (Mikaelyan *et al*., 2015b). It represents a separate line of descent in the *Treponema* complex that comprises the free-living *Treponema caldarium* and *Treponema stenostreptum* (Lilburn *et al*., 1999; Ohkuma *et al*., 1999; Abt *et al*., 2013). The other clade, which has been referred to as 'termite *Treponema* cluster II' (Ohkuma *et al*., 1999; Noda *et al*., 2003), hereafter 'termite cluster

Received 18 March, 2021; revised 12 May, 2021; accepted 13 May, 2021. *For correspondence. E-mail brune@mpi-marburg.mpg.de; Tel. +49-6421-178-101; Fax +49-6421-178-999.

II', is much less diverse and more closely related to the *Treponema* species associated with other animals. Its members occur only in a few evolutionary lower termites, where they are associated with certain gut flagellates but are absent from all higher termites (fam. Termitidae) (Iida *et al*., 2000; Noda *et al*., 2018).

The only termite gut treponemes cultured to date are representatives of termite cluster I and have been isolated from lower termites. The first isolate, *Treponema primitia*, is a homoacetogen capable of reductive acetogenesis from $H_2 + CO_2$ via the Wood–Ljungdahl pathway (Leadbetter *et al*., 1999; Graber and Breznak, 2004). Gene inventories of key enzymes of the bacterial Wood–Ljungdahl pathway, namely, formyltetrahydrofolate synthetase (FTHFS; Salmassi and Leadbetter, 2003; Pester and Brune, 2006; Warnecke *et al*., 2007; Ottesen and Leadbetter, 2010, 2011), the formate dehydrogenase subunit (FDH_H) of the hydrogen-dependent carbon dioxide reductase (HDCR; Zhang *et al*., 2011; Zhang and Leadbetter, 2012), and the beta-subunit (CooS) of the CO dehydrogenase/acetyl-CoA synthase complex (Warnecke *et al*., 2007; Matson *et al*., 2011), showed that homologues from termite gut treponemes are abundantly represented in various wood-feeding lower or higher termites (including the wood-feeding cockroach *Cryptocercus punctulatus*, the closest relative of termites), but not in omnivorous cockroaches.

Although these findings suggest that termite gut treponemes play an important role in reductive acetogenesis, which is the most important hydrogen sink in termite guts (Brune, 2014), the distribution of the capacity for reductive acetogenesis among the mostly uncultured members of termite cluster I is entirely unclear. Unlike *T. primitia*, the other species in termite cluster I, *Treponema azotonutricium* (Lilburn *et al*., 2001; Graber *et al*., 2004) and *Treponema isoptericolens* (Dröge *et al*., 2008), are not acetogens but rather classical sugar fermenters. Moreover, the gene inventories are potentially misleading because elements of the Wood–Ljungdahl pathway occur also in non-acetogenic organisms, where they are involved in the assimilation and interconversion of C_1 metabolites (Drake, 1994).

Importantly, a complete Wood–Ljungdahl pathway occurs also in *Candidatus* Treponema intracellularis, the only identified member of termite cluster II (Ohkuma *et al*., 2015), and in *Candidatus* Adiutrix intracellularis, the first representative of a deep-branching clade of *Deltaproteobacteria* (Ikeda-Ohtsubo *et al*., 2016); these two uncultured endosymbionts of termite gut flagellates contribute substantially to the high rates of reductive acetogenesis from $H_2 + CO_2$ in the hindgut of their respective termite host (Rosenthal *et al*., 2013; Ohkuma *et al*., 2015). Although these bacteria represent lines of descent that are different from *T. primitia*, all possess key genes of the Wood–Ljungdahl pathway that are closely related to homologues from *Firmicutes*, which indicates that the capacity for reductive acetogenesis has been independently acquired by lateral gene transfer (Salmassi and Leadbetter, 2003; Matson *et al*., 2011; Ikeda-Ohtsubo *et al*., 2016). Consequently, it remains unsettled whether the putative ancestor of termite cluster I, which was probably present already in the common ancestor of *Cryptocercus* and termites, was already acetogenic, or whether this trait was acquired - possibly even more than once - only in individual lineages.

Almost nothing is known about the presence of treponemes in cockroaches. Members of termite clusters I and II were detected, albeit in low abundance, in short-read amplicon libraries of the bacterial gut microbiota of various cockroaches, including the wood-feeding *Cryptocercus punctulatus* (Dietrich *et al*., 2014; Schauer *et al*., 2014; Tai *et al*., 2015; Berlanga *et al*., 2016; Lampert *et al*., 2019). However, none of these phylotypes were represented in any of the 16S-rRNA-based clone libraries of the bacterial gut microbiota of cockroaches (Schauer *et al*., 2012; Bauer *et al*., 2015; Mikaelyan *et al*., 2015b), and their phylogenetic relationship to termite gut treponemes remains unclear.

Here, we report the isolation of the first representative of termite cluster I from the gut of an omnivorous Madeira cockroach (*Rhyparobia maderae*), using a combination of membrane filtration and deep-agar dilution series. We conducted a detailed ultrastructural and physiological characterization of strain RmG30, including its response to oxygen, and investigated its relationship to members of the termite cluster I and other members of the family *Treponemataceae* by phylogenomic analysis.

Results

Morphological characterization

Strain RmG30 showed visible growth in anoxic deep-agar tubes after 2 weeks of incubation. Initially, the colonies (<0.1 mm in diameter) had an irregular shape, but after 3 weeks, they became spherical with a well-defined edge (~0.2 mm in diameter). After 2–3 months, the colonies were white and cotton-ball-like with blurred edges and had a diameter of approximately 1–2 mm.

Phase-contrast microscopy of liquid cultures showed spiral-shaped cells with a length of 10–25 (some 3–90) μm (Fig. 1A). Cells were highly motile. Spherical bodies with a diameter of 2–4 μm were present in all cultures and increased in abundance during the stationary phase (Fig. 1B). Scanning electron microscopy revealed a cell width of 0.20 ± 0.01 μm and a wavelength of 1.0 ± 0.1 (some 0.8–1.6) μm (Fig. 1C). Transmission electron microscopy of ultrathin sections rarely showed two,

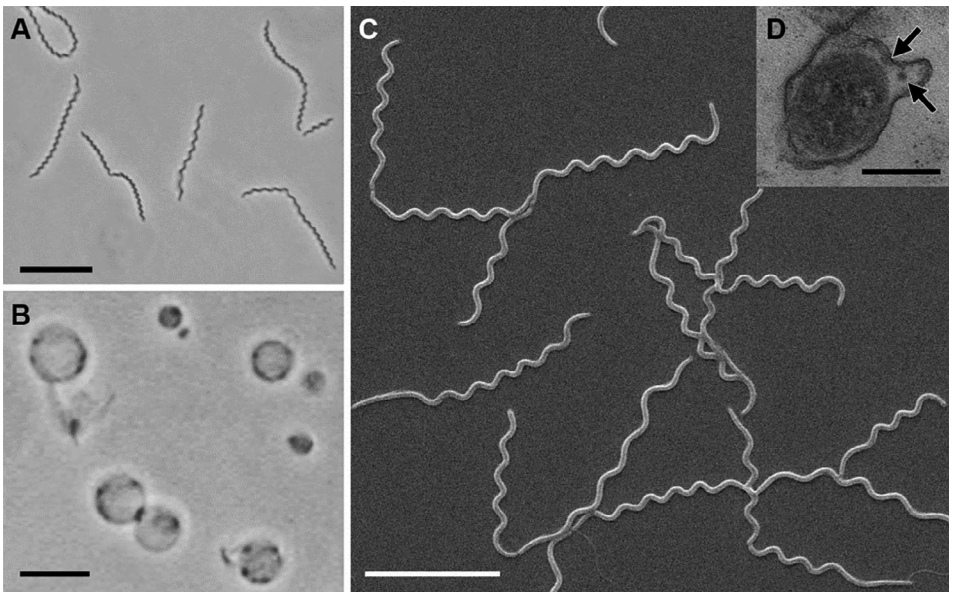

Fig 1. Morphology and ultrastructure of strain RmG30. Phase-contrast micrographs of cells in a growing culture (A) and spherical bodies formed in the stationary phase (B); scanning electron micrograph of cells in a growing culture (C); transmission electron micrograph of the cross-section of a cell (D); the arrows indicate the periplasmic flagella. Scale bars are 10 μm (A), 5 μm (B, C) and 0.2 μm (D).

typically one, and sometimes no periplasmic flagella, indicating that the cells possess single periplasmic flagella at each end that do not always overlap at mid-cell (Fig. 1D).

Phylogenetic analyses

16S rRNA gene sequence analysis indicated that strain RmG30 falls into the radiation of the genus *Treponema* (Fig. 2). It represents a novel lineage that is the most basal member of termite cluster I. Together with *T. caldarium* and *T. stenostreptum*, they form a well-supported family-level clade that occupies a sister position to all other members of the genus *Treponema* (family *Treponemataceae*).

A phylogenomic analysis of all members of the order *Spirochaetales* with sequenced genomes confirmed the basal position of strain RmG30 in termite cluster I (Fig. 3 and Supplementary Fig. S1). As in the 16S rRNA-based analysis, the strain represents a line of descent that is separate from those of *T. primitia* and *T. azotonutricium* (the genome of *T. isoptericolens* has not been sequenced), and from numerous MAGs from higher termites (Hervé *et al*., 2020). The sister position of the ectosymbiotic spirochete of *Oxymonas* sp. from *Neotermes koshunensis* (NkOx-clu11) to *T. primitia* agrees with the original report (Utami *et al*., 2019). Notably, a MAG from the fungus-cultivating termite *Macrotermes natalensis* does not cluster with other MAGs from higher termites but represents the same lineage as strain RmG30.

The sequence similarities between the 16S rRNA genes of RmG30 and the other species of the clade range between 90.6% and 93.2% (Fig. 4), which is below the threshold typically observed among members of the same genus (Yarza *et al*., 2014). Likewise, the low average nucleotide identities between the genomes of strain RmG30 and the corresponding type strains (Fig. 4) justifies to consider each species a separate genus-level taxon. This agrees with the results obtained with the GTDB toolkit (Chaumeil *et al*., 2020), which classified *T. caldarium*, strain RmG30, and the termite gut isolates (*T. primitia* and *T. azotonutricium*) as separate genera in the family 'Treponemataceae_B' and elevated the family *Treponemataceae* to an order-level lineage ('Treponematales') separate from the other families in the *Spirochaetales* (Fig. 3; Supplementary Table S1). Also, members of the genus *Rectinema* (which are currently assigned to *Treponemataceae*; Hördt *et al*., 2020) were identified as a separate, family-level lineage (f__UBA8932) in the order 'Treponematales'.

Growth and physiology

Strain RmG30 grew at temperatures between 20 and 37°C, with the highest growth rate at 35°C; growth yields showed a broad optimum between 25 and 35°C (Fig. 5A). The pH range of growth was between 6.5 and 7.8, with a broad optimum above pH 7.3 (Fig. 5B). Growth yields decreased drastically as soon as the pH fell below 7.3. Doubling times were similar above pH 7 (16–18 h) but increased at lower pH. Acid production stopped at a final pH of 6.0. No growth occurred at pH 8.5 (not shown).

Strain RmG30 grew fermentatively on D-glucose and a variety of other carbohydrates, including D-mannose, D-galactose, D-fructose, D-xylose, L-arabinose, D-ribose, D-trehalose and *N*-acetyl-glucosamine. Liquid culture on glucose showed no lag phase and reached maximal

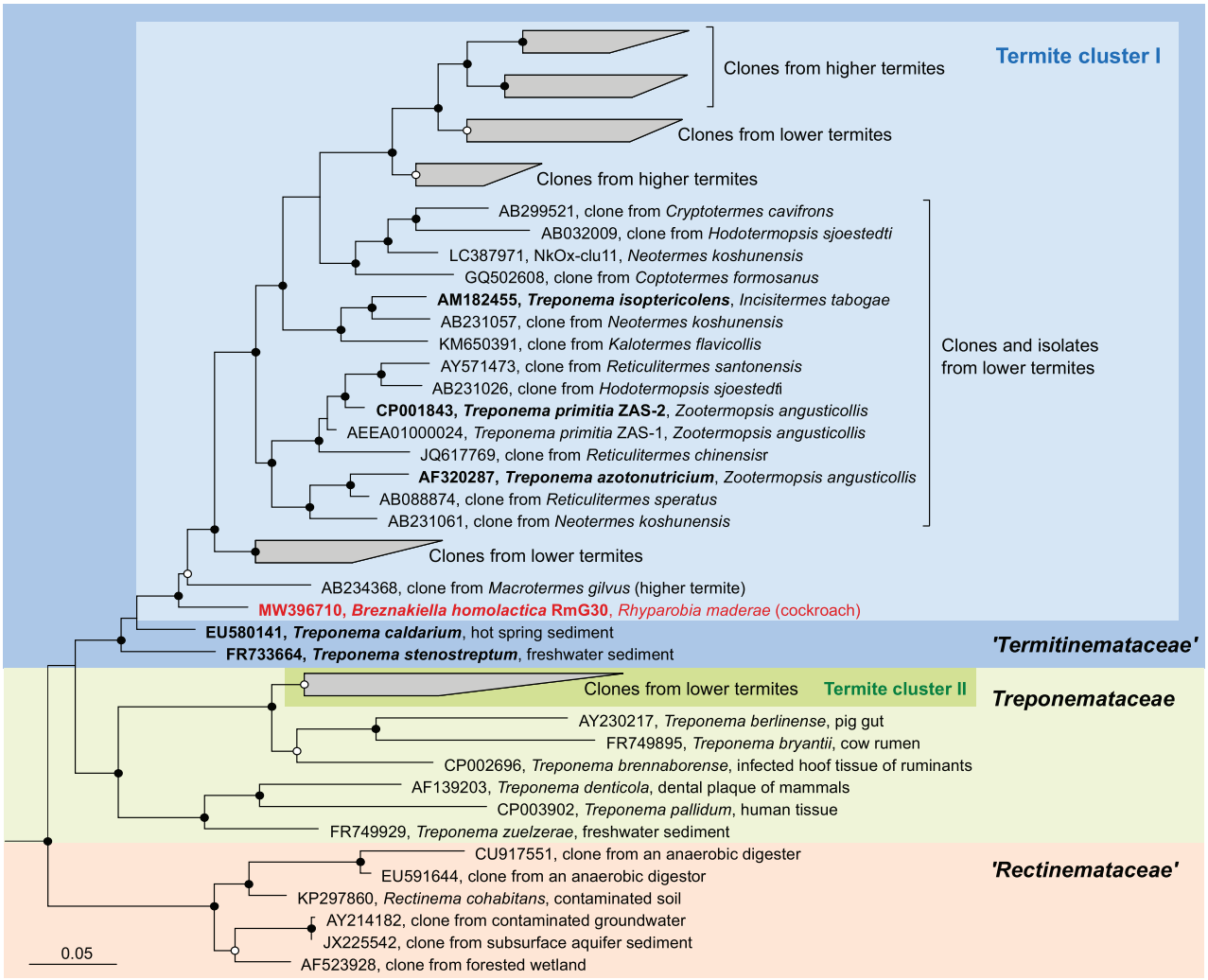

Fig 2. 16S rRNA gene tree illustrating the relationship of strain RmG30 (red) to other lineages of termite cluster I and other members of the family *Treponemataceae*. Type strains that represent genus-level taxa in the newly proposed family '*Termitinemataceae*' are shown in bold. Members of *Spirochaetaceae* were used as outgroup. Bullets indicate node support (● ≥ 95%; ◦ ≥ 70%). [Color figure can be viewed at wileyonlinelibrary.com]

turbidity within 10 days. Cells precultivated on glucose showed a lag phase of 7–14 days when transferred on D-mannose, D-ribose and D-trehalose, and a lag phase of 14–28 days on D-galactose, D-fructose, L-arabinose and *N*-acetyl-glucosamine, indicating that the corresponding pathways require induction. No growth was observed on L-rhamnose, D-mannitol, D-gluconic acid, D-glucuronic acid, D-cellobiose, D-maltose, D-sucrose, D-lactose, starch, cellulose, xylan, pyruvate, L-lactate, formate and $H_2 + CO_2$.

Lactate was the only product detected from all sugars tested. Acetate was formed only from *N*-acetyl-glucosamine and in stoichiometric amounts, indicating that it stems exclusively from deacetylation (Table 1). Ethanol, formate, or H_2 were not detected, and carbon and electron recoveries were complete on all substrates. The lactate-to-substrate stoichiometries on glucose (1.96), *N*-acetyl-glucosamine (2.08) and xylose (1.73) matched those expected from homolactic fermentation of hexoses (2.00) and pentoses (1.67). Growth rates on xylose and *N*-acetyl-glucosamine were close to those on glucose, but growth yields were higher on *N*-acetyl-glucosamine and lower on xylose (Table 1).

Fumarate was not reduced to succinate in the presence of glucose, formate, or H_2. The addition of H_2 to the headspace did not affect growth and product formation on glucose. Cells did not grow in mineral medium without yeast extract and Casamino acids. Higher concentrations of yeast extract (0.2%) slightly stimulated the growth.

Strain RmG30 grew in non-reduced anoxic medium under N_2/CO_2, but no growth occurred if 0.5% O_2 was added to the headspace. Catalase and oxidase activity

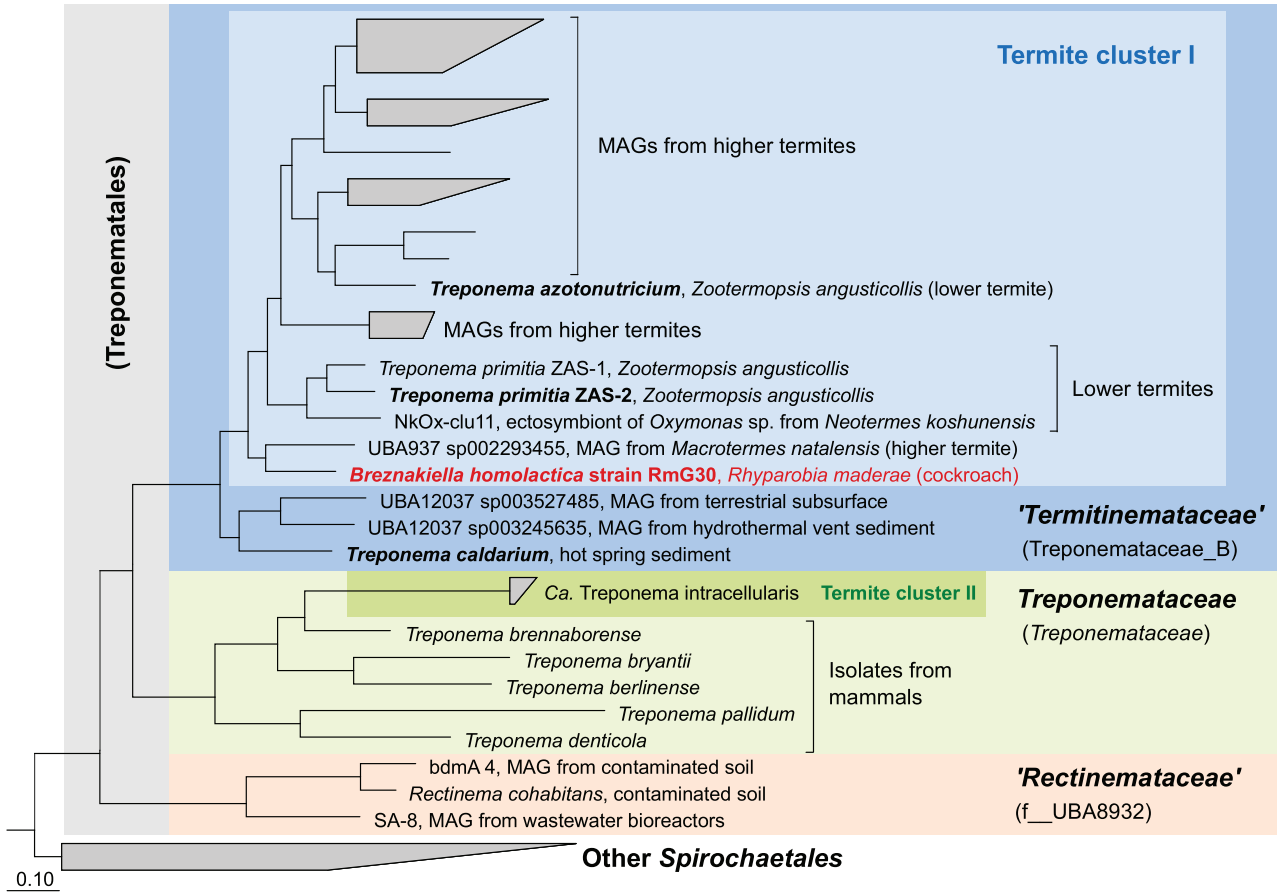

Fig 3. Phylogenomic tree illustrating the relationship of strain RmG30 (red) to termite cluster I and other members of the family *Treponemataceae*. Type strains that represent genus-level lineages in the newly proposed family '*Termitinemataceae*' are shown in bold. All nodes in the tree are fully supported (>99%). The tree was rooted using other lineages of *Spirochaetia* as outgroup. Taxon names that differ in the GTDB taxonomy are shown in parentheses. For a fully expanded version of the tree, including genome accession numbers, see Supplementary Fig. S1. The detailed results of the GTDB-tk classification are shown in Supplementary Table S1. [Color figure can be viewed at wileyonlinelibrary.com]

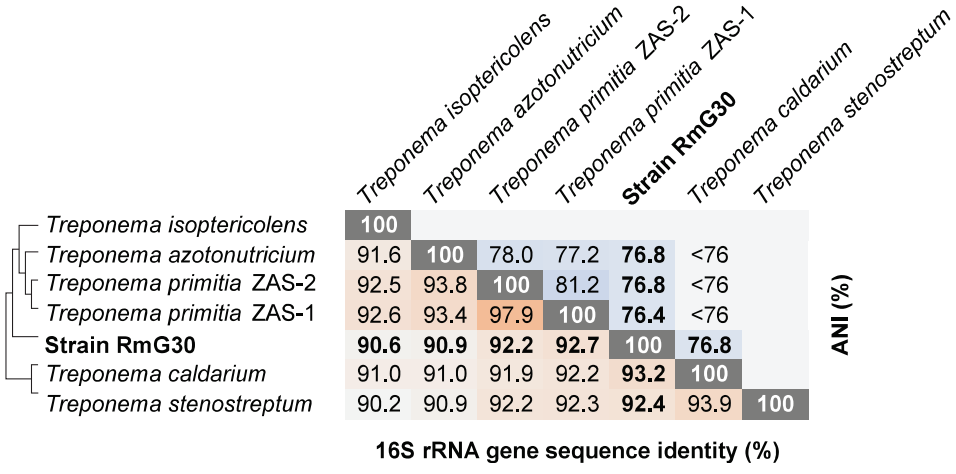

Fig 4. Pairwise comparison of sequence identity of the 16S rRNA genes and average nucleotide identity (ANI) of the genomes between strain RmG30 and its relatives in the proposed family '*Termitinemataceae*'. The phylogenetic relationship was taken from Fig. 2. The colour depth of each cell was adjusted according to the respective value. ANI values <76% are below the cut-off of the FastANI tool. [Color figure can be viewed at wileyonlinelibrary.com]

were not detected in cells grown on standard medium. However, cultures amended with hemin showed catalase activity. In washed cell suspensions incubated in the presence of oxygen, the turnover rate of glucose was significantly higher (0.99 ± 0.03 μmol mg^{-1} h^{-1}) than under anoxic conditions (0.70 ± 0.08 μmol mg^{-1} h^{-1}), and acetate accumulated (0.12 ± 0.01 μmol mg^{-1} h^{-1}) in addition to lactate (Fig. 6). The amount of air that had to

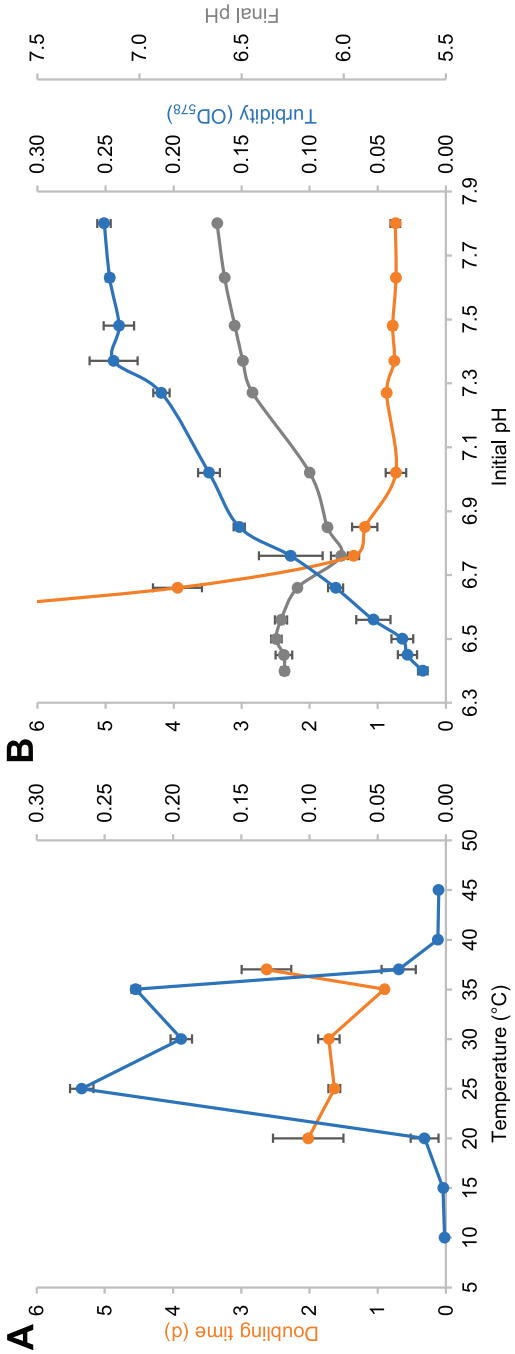

Fig 5. Influence of temperature and pH on doubling time and growth yield (OD_{578}) of strain RmG30. Cells were grown in basal medium on 8 mM glucose. For temperature dependence (A), the initial pH was 7.0. For pH dependence (B), the initial pH was adjusted by adding different volumes of CO_2 to the culture headspace. The final pH of the cultures was recorded in the stationary phase. Values are means of three cultures (±standard deviation). [Color figure can be viewed at wileyonlinelibrary.com]

be added to the tubes to maintain microoxic conditions indicated a considerable rate of O_2 consumption (roughly estimated at 0.2–0.3 μmol mg^{-1} h^{-1}).

Genome analysis

Genome assembly of strain RmG30 resulted in a circular genome with a genome size of 4 646 109 bp and a G + C content of 52.9 mol.%. Exploration of the annotated genes (Supplementary Table S2) fully explained the substrate spectrum of the strain and revealed further details of its homolactic metabolism (Fig. 7).

The genome encodes two possible mechanisms for the uptake and activation of glucose: (i) via glucose permease (GlcU) plus hexokinase, and (ii) via a phosphotransferase system (PTS) of the Man family, whose members have been shown to transport and phosphorylate glucose, mannose, fructose, *N*-acetyl-glucosamine and other substrates in *E. coli* (Plumbridge and Vimr, 1999). In addition, the genome contains numerous genes encoding putative transporters, including putative ATP-binding cassette transporters for galactose, xylose, ribose and trehalose, and putative major facilitator superfamily transporters for arabinose.

The glycolytic pathway oxidizing hexose phosphates to pyruvate is complete. The absence of glucose 6-phosphate dehydrogenase and phosphoketolase agree with the homolactic fermentation of both hexoses and pentoses. The absence of transaldolase, which catalyses a key step in the pentose phosphate pathway, indicates that pentoses are most likely shuttled into glycolysis via a bypass of the classic pentose phosphate pathway, which has been experimentally documented in *E. coli* mutants lacking transaldolase (Nakahigashi *et al.*, 2009). It involves the phosphorylation of sedoheptulose 7-phosphate to sedoheptulose 1,7-bisphosphate and its subsequent cleavage to erythrose 4-phosphate and dihydroxyacetone phosphate. These activities are side reactions of 6-phosphofructokinase and fructose 1,6-bisphosphate aldolase, which are represented in the genome of strain RmG30 in multiple copies (Supplementary Table S2).

The genome encodes a D-lactate dehydrogenase required to reduce pyruvate to lactate. In addition, there are homologues encoding pyruvate formate lyase (PFL) and pyruvate:ferredoxin oxidoreductase (PFOR), which catalyse the conversion of pyruvate to acetyl-CoA, enzymes for the production of ethanol (acetaldehyde dehydrogenase, alcohol dehydrogenase) and acetate (phosphate acetyltransferase, acetate kinase), and two [FeFe] hydrogenases, namely, a ferredoxin- and NAD^+-dependent electron-bifurcating hydrogenase (HydABC) of group A and a ferredoxin-dependent homologue of group B (HydA2). The genome also encodes a ferredoxin:

Table 1. Growth parameters and fermentation balance of strain RmG30 on different substrates.

Substrate	Substrate consumed (mM)	Doubling time (h)	Turbidity (OD_{578})	Yield coefficient (g mol^{-1})[a]	Substrate assim. (mM)[b]	Products formed (mM) Lactate	Acetate	Carbon and electron recovery (%)[c]
No substrate			0.023[d]			1.5[d]	–	
Glucose	8.0	16	0.202	13.5	0.7	15.8	–	99
Xylose	8.0	14	0.142	9.0	0.6	14.3	–	104
N-Acetyl-glucosamine[e]	8.0	15	0.247	16.8	0.9[f]	16.3	8.1	105

Unless indicated otherwise, precultures were grown on glucose. Values are means of results obtained with duplicate cultures (less than 10% deviation).
[a]Based on consumed substrate and the conversion factor determined for glucose-grown cultures (60 ± 2 mg L^{-1} at $OD_{578} = 0.1$; $n = 2$).
[b]Assuming an elemental composition of $C_4H_8O_2N$ for bacterial cell mass (Mayberry *et al*., 1968).
[c]Based on dissimilated substrate.
[d]Turbidity and products formed in basal medium without glucose were subtracted in the subsequent calculations.
[e]Preculture grown on *N*-acetyl-glucosamine.
[f]Calculated as assimilated glucose.

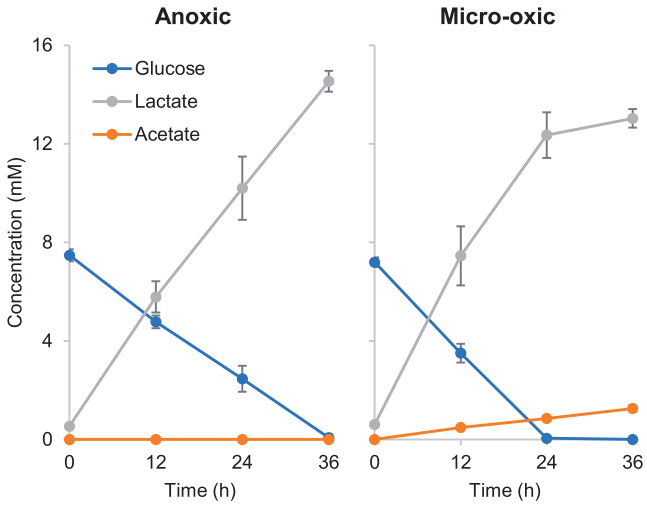

Fig 6. Effect of oxygen on glucose turnover by cell suspensions of strain RmG30. Washed cells (0.3 mg ml^{-1}) were incubated under a headspace of N_2/CO_2 under anoxic (1 mM DTT) or microoxic (0.2%–0.4% O_2) conditions. Values are means of four cultures (±standard deviation). [Color figure can be viewed at wileyonlinelibrary.com]

$NADP^+$ oxidoreductase (FNR) and a Na^+-translocating ferredoxin:NAD^+ oxidoreductase (Rnf) complex.

Key enzymes of the Wood–Ljungdahl pathway (hydrogen-dependent CO_2 reductase (HDCR), carbon monoxide dehydrogenase/acetyl-CoA synthase (CODH/ACS)) are absent, confirming the inability of strain RmG30 to catalyse reductive acetogenesis. Genes indicating the capacity for aerobic respiration or anaerobic respiration with sulfate or nitrate as electron acceptor were not detected. The genome encodes several homologues of succinate dehydrogenase/fumarate reductase, although we found no evidence for fumarate respiration in strain RmG30 (see above). Genes encoding pyruvate oxidase, catalase and peroxiredoxin are present, but homologues of superoxide dismutase and glutathione peroxidase were not found.

Strain RmG30 possesses transporters for peptides, amino acids and ammonia (Supplementary Table S2). It encodes the biosynthetic pathways for almost all proteinogenic amino acids (Supplementary File 1). The pathway for tryptophan synthesis is absent. Meso-diaminopimelate, an essential precursor of lysin and peptidoglycan, is probably synthesized directly from tetrahydrodipicolinate via diaminopimelate aminotransferase (DapL) (McCoy *et al*., 2006), but all possible pathway variants lack at least one coding gene, it is unclear whether strain RmG30 can synthesize lysine (Supplementary Fig. S2). In the case of methionine synthesis, the acylhomoserine pathway that is used by most bacteria is incomplete, but strain RmG30 might produce homocysteine via an aspartate semialdehyde sulfur transferase (Ast, Supplementary Fig. S2), as experimentally documented in methanogenic archaea (Allen *et al*., 2015). The pathways for the synthesis and breakdown of glycogen are complete, which indicates that strain RmG30 uses glycogen as an intracellular reserve compound. Genes encoding homologues of group IV nitrogenases (structural subunits D, H and K) are most likely not involved in dinitrogen fixation but seem to be part of an Fe^{3+}-siderophore transport system (Supplementary Table S2; Ghebreamlak and Mansoorabadi, 2020).

Discussion

The isolation of the most basal member of termite cluster I from a cockroach provides important insights into the metabolic diversity of this clade and the evolutionary history of termite gut treponemes. Like the termite gut

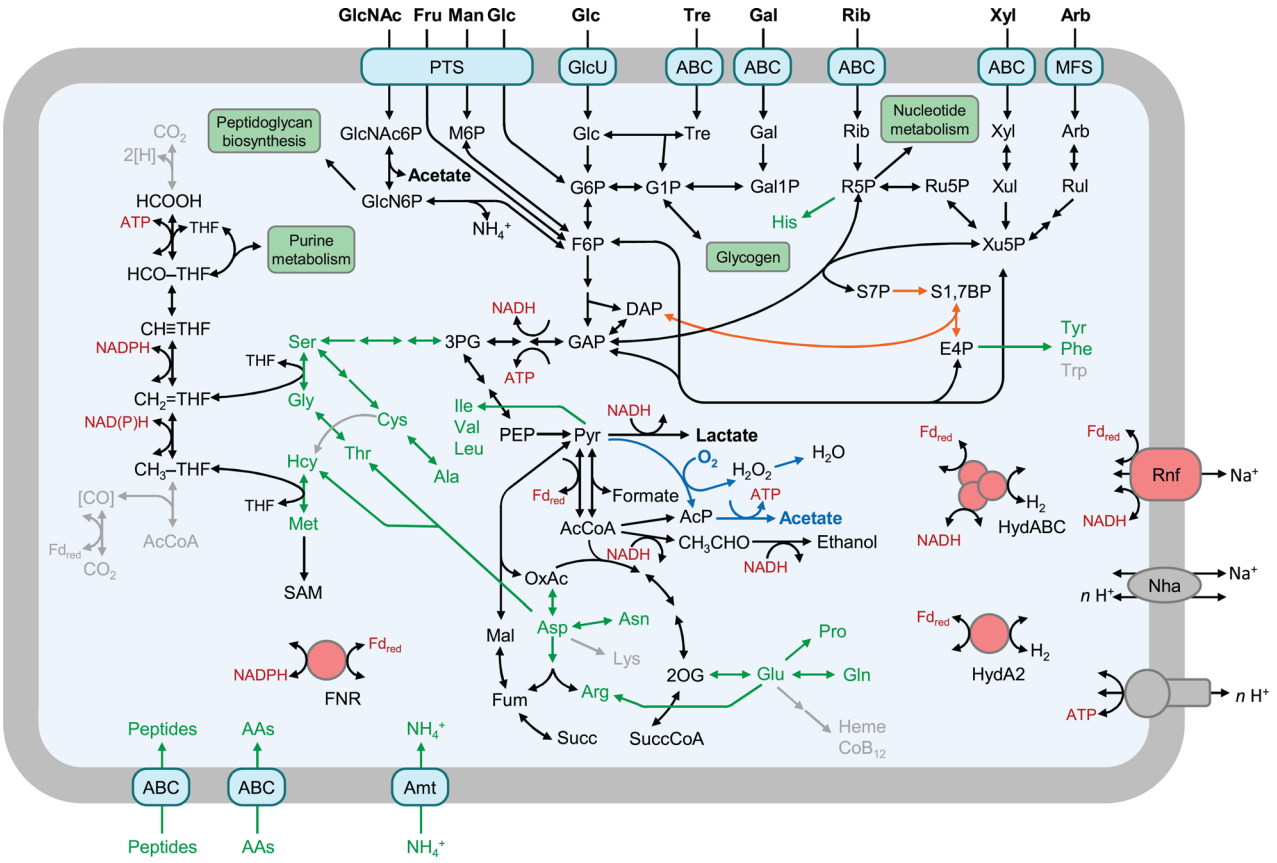

Fig 7. Metabolic map of strain RmG30. Substrates and products that were experimentally verified are shown in bold. The hypothetical bypass in the pentose phosphate pathway compensating for the absence of transaldolase (see text) is shown in orange. The pathway for the oxygen-dependent production of acetate is shown in blue. Missing reactions are shown in grey. Important cosubstrates in energy metabolism are shown in red. Amino acids (AAs) and their biosynthetic pathways are outlined in green. Non-standard abbreviations (non-IUPAC) for metabolites: Ac, acetate; AcCoA, acetyl coenzyme A; AcP, acetyl phosphate; Ara, arabinose; CoB_{12}, Coenzyme B_{12}; DAP, dihydroxyacetone phosphate; E4P, erythrose 4-phosphate; Fru, fructose; F6P, fructose 6-phosphate; Fum, fumarate; Gal, galactose; Gal1P, galactose 1-phosphate; GAP, glyceraldehyde 3-phosphate; Glc, glucose; G1P, glucose 1-phosphate; G6P, glucose 6-phosphate; GlcNAc, N-acetyl-glucosamine; GlcNAc6P, N-acetyl-glucosamine 6-phosphate; GlcN6P, glucosamine 6-phosphate; Hcy, homocysteine; Mal, malate; Man, mannose; M6P, mannose 6-phosphate; 2OG, 2-oxoglutaric acid; OxAc, oxaloacetate; PEP, phosphoenolpyruvate; 3PG, 3-phosphoglycerate; Pyr, pyruvate; Rib, ribose; R5P, ribose 6-phosphate; Rul, ribulose; Ru5P, ribulose 5-phosphate; SAM, S-adenosyl methionine; S7P, sedoheptulose 7-phosphate; S1,7BP, sedoheptulose 1,7-bisphosphate; Succ, succinate; SuccCoA, succinate coenzyme A; THF, tetrahydrofolate; Tre, trehalose; Xul, xylulose; Xu5P, xylulose 5-phosphate; Xyl, xylose; for enzymes and transporters: ABC, ATP-binding cassette transport system; Amt, ammonium transporter; FNR, ferredoxin:$NADP^+$ oxidoreductase; GlcU, glucose uptake protein; HydABC, ferredoxin- and NAD^+-dependent electron-bifurcating [FeFe]-hydrogenase; HydA2, ferredoxin-dependent [FeFe]-hydrogenase; MFS, major facilitator superfamily transporter; Nha, Na^+/H^+ antiporter; PTS, phosphotransferase system; Rnf, Na^+-translocating ferredoxin:NAD^+ oxidoreductase complex. [Color figure can be viewed at wileyonlinelibrary.com]

isolates *T. azotonutricium* and *T. isoptericolens*, strain RmG30 possesses a purely fermentative metabolism and lacks the ability to grow lithotrophically on $H_2 + CO_2$ (or homoacetogenically on glucose), corroborating the hypothesis that the capacity for reductive acetogenesis in *T. primitia* has been acquired by lateral gene transfer from *Firmicutes* (Salmassi and Leadbetter, 2003; Matson *et al*., 2011; Ikeda-Ohtsubo *et al*., 2016). Moreover, the inability to grow on xylan agrees with the hypothesis that also the hemicellulolytic capacity attributed to uncultured members in the apical lineages of termite cluster I, which occur exclusively in higher termites, was acquired by lateral gene transfer (Tokuda *et al*., 2018).

Evolutionary history of termite cluster I

Members of termite cluster I are present in all termite species investigated so far and - unlike the cellulolytic flagellates - even maintained a prominent place in the microbial community after the evolutionary transition from a protist-based (lower termites) to a bacteria-based (higher termites) digestion of lignocellulose (Brune and Dietrich, 2015; Chouvenc *et al*., 2021). The internal phylogeny of the clade provides a strong coevolutionary signal with the major host groups (Mikaelyan *et al*., 2015b; Bourguignon *et al*., 2018), but their evolutionary origin is entirely obscure.

It is widely accepted that termites evolved from wood-feeding, subsocial cockroaches (Bourguignon *et al*., 2015). Although the gut microbiota of cockroaches and termites shows a strong coevolutionary pattern (Dietrich *et al*., 2014) and the presence of particular taxa is linked to host diet (Mikaelyan *et al*., 2015a), concrete evidence for an origin of termite gut treponemes in an ancestral cockroach is so far lacking.

Hence, the genome sequence of strain RmG30 is of great significance for the reconstruction of the evolutionary history of termite cluster I. The monophyly of the cluster, its exclusive presence in termites, and the striking host specificity of its members (the phylotypes from a particular termite species are, in general, more closely related to each other than to any phylotype from other termites), had been recognized already in the early studies of termite gut treponemes (Lilburn *et al*., 1999; Ohkuma *et al*., 1999). Our phylogenomic analysis, corroborated by the corresponding 16S rRNA-based phylogeny, provides unequivocal support for a basal position of strain RmG30 (from a cockroach), an intermediate position of the isolates from lower termites, and an apical position of clones (there are no isolates) from higher termites, which is in full agreement with a coevolutionary scenario (Fig. 2).

An interesting exception is the single clone (AB234368) obtained from *Macrotermes gilvus* (Hongoh *et al*., 2006) and a corresponding MAG (g__UBA937) from *Macrotermes natalensis* (Parks *et al*., 2017), which are more closely related to strain RmG30 than to all other members of termite cluster I. Apparently, the fungus-feeding *Macrotermes* spp. have independently acquired a lineage of termite cluster I that is separate from the main line of descent - possibly from a cockroach. This was corroborated by phylogenetic placement of the short reads previously obtained from amplicon libraries of cockroach gut microbiota (Lampert *et al*., 2019), where reads from several cockroaches that had been classified as *Treponema caldarium* or termite cluster I clustered with the 16S rRNA gene of strain RmG30 and the clone from *Macrotermes gilvus* (details not shown). Such a horizontal acquisition of termite gut microbiota from the environment, including the guts of other animals, is not unusual (Bourguignon *et al*., 2018), and agrees with the observation that the gut microbiota of Macrotermitinae (fungus-feeding higher termites) is more similar to that of cockroaches than to termites from other diet groups (Dietrich *et al*., 2014; Otani *et al*., 2014; Lampert *et al*., 2019).

These observations provide strong evidence that members of termite cluster I were already present among the gut microbiota of omnivorous cockroaches before the common ancestor of termites and Cryptocercidae acquired cellulolytic flagellates. Since *Rhyparobia maderae* (superfam. Blaberoidea), the host of strain RmG30, is only distantly related to the lineage that gave rise to termites (superfam. Blattoidea) (Djernæs *et al*., 2020), host specificity and transmission mode of the basal members of termite cluster I in cockroaches remain unclear. The same is true for the ultimate origin of the cluster and their relationship to the isolates from freshwater sediments (*T. stenostreptum* and *T. caldarium*). Clearly, more information is needed on the diversity and distribution of the cluster in cockroaches, other insects and their environments.

Energy metabolism

Since the isolation of *T. primitia* (Leadbetter *et al*., 1999; Graber *et al*., 2004), evidence has accumulated that members of termite cluster I are responsible for the high rates of reductive acetogenesis in termite guts. However, *T. primita* and possibly also the closely related strain NkOx-clu11, an uncultured ectosymbiont of a termite gut flagellate, are the only representatives of the cluster that possess a complete Wood–Ljungdahl pathway (Rosenthal *et al*., 2011; Utami *et al*., 2019). Their energy metabolism resembles that of *Acetobacterium woodii* and involves an HDCR, a CODH/ACS complex, an electron-bifurcating hydrogenase (HydABC), and an Rnf complex, which balance the reducing equivalents and generate the membrane potential for ATP synthesis (Schuchmann and Müller, 2014).

The presence of a fermentative metabolism in the ancestral *T. caldarium* and *T. stenostreptum*, in strain RmG30, and in two of the three species isolated from termite guts is a strong indication that reductive acetogenesis in *T. primitia* and possibly other uncultured members of termite cluster I is an apomorphic trait. This agrees with the absence of HDCR and CODH/ACS from *T. azotonutricium* and strain RmG30 - the only other isolates of termite cluster I with sequenced genomes - and from the MAG from *Macrotermes natalensis*, the closest relative of strain RmG30 in the phylogenomic tree (Fig. 3). The gene functions of the Wood–Ljungdahl pathway that are encoded by strain RmG30 (Fig. 7) and all other basal members of the clade probably serve in the interconversion of C_1 compounds and the provision of formate and methyl groups for the biosynthesis of purines (Sah *et al*., 2015), methionine and serine (Zhuang *et al*., 2014) and were most likely present already in the common ancestor of termite cluster I. The Wood–Ljungdahl pathway was most likely complemented during the radiation of the clade by the lateral acquisition of HDCR and CODH/ACS from acetogenic *Firmicutes*, rendering certain lineages acetogenic. It remains to be clarified whether this has happened more than once.

There is circumstantial evidence that also the apical lineages of termite cluster I, which occur exclusively in higher termites (Fig. 3), may not be acetogenic.

Metagenome analysis of the hindgut fluid of a *Nasutitermes* sp. revealed numerous gene homologues encoding FTHFS and CODH/ACS that were assigned to treponemes, but homologues of HDCR were conspicuously absent (Warnecke *et al*., 2007). Comparative analysis of the gene functions encoded by the uncultured representatives of termite cluster I, including also MAGs from lower termites, will allow to clarify the situation (Y. Song, V. Hervé, and A. Brune; unpublished results).

An unusual feature of strain RmG30 is the homolactic fermentation of pentoses. While homolactic fermentation which uses the glycolytic pathway and yields two lactate per sugar, is typical for hexoses, pentoses are usually fermented heterolactically via the phosphoketolase pathway, which yields one lactate and one acetate (Kandler, 1983). Homolactic fermentation of pentoses is quite rare in nature but common in biotechnological applications, where a high yield of lactate is achieved by genetic engineering (Tarraran and Mazzoli, 2018), which usually involves the substitution of phosphoketolase with a heterologous expressed transketolase (Okano *et al*., 2009).

The absence of both phosphoketolase and transaldolase from the genome of strain RmG30 and the formation of about 1.7 lactate per xylose, which matches the theoretical stoichiometry of a homolactic fermentation, indicates that pentoses are converted to hexoses via a modified pentose phosphate pathway that involves a sedoheptulose 1,7-bisphosphate shunt (Nakahigashi *et al*., 2009; see above). While the few lactic acid bacteria that ferment pentoses via pentose phosphate pathway/glycolysis still form appreciable amounts of acetate, strain RmG30 is the first strain that conducts a purely homolactic fermentation of pentoses. Although the strain has the genomic capacity to convert pyruvate to acetyl-CoA (via PFL or PFOR) and to form acetate, formate, hydrogen or ethanol, these enzymes are obviously not involved in catabolic reactions.

Relationship to oxygen

Insect guts are gradient systems characterized by the continuous influx of oxygen across the gut epithelium (Brune, 2014). Therefore, even strictly anaerobic members of the gut microbiota may be at least temporarily exposed to oxygen. Typical adaptations to microoxic conditions are pathways for a non-respiratory reduction of oxygen and the removal of reactive oxygen species, which can be found even in strict anaerobes (e.g. Condon, 1987; Brioukhanov and Netrusov, 2007; Imlay, 2019). Strain RmG30 is no exception. Although it has a purely fermentative metabolism and does not grow under microoxic conditions (0.5% O_2, vol./vol.), resting cells consume oxygen and accumulate acetate at appreciable rates. An oxygen-dependent accumulation of acetate is common among lactic acid bacteria, which reduce oxygen in non-respiratory pathways, which shifts fermentation products from lactate to acetate and allows to gain additional ATP (e.g. Condon, 1987; Bauer *et al*., 2000). In strain RmG30, oxygen consumption is most likely catalysed by pyruvate oxidase; homologues of lactate oxidase or NADH oxidase were not detected.

Like most non-respiratory oxidases, pyruvate oxidase produces acetyl-CoA and H_2O_2. The latter is cytotoxic but may be detoxified by catalase, which ameliorates the effects of H_2O_2 production and increases oxygen tolerance (Whittenbury, 1960; Engesser and Hammes, 1994). Also, the genome of strain RmG30 encodes the apoenzyme, catalase activity requires the presence of hemin. The dependence of catalase activity on an external hemin supply is common in lactic acid bacteria (Baureder and Hederstedt, 2013) but has been reported also for methanogens (Brioukhanov and Netrusov, 2012). In strain RmG30, hemin auxotrophy is explained by the absence of genes required for porphyrin biosynthesis, which indicates a requirement also for vitamin B_{12}. Such cross-feeding of growth factors is common in gut environments (Sokolovskaya *et al*., 2020), exemplified by the dependence of *T. primitia* on the provision of folinate by other members of the termite gut microbiota (Graber and Breznak, 2005).

Except for the microaerophilic *Treponema pallidum*, which requires low levels of oxygen for survival and multiplication, all other members of the genus *Treponema* are considered strict anaerobes (Norris *et al*., 2015). Nevertheless, cultures of *T. primitia* tolerate exposure to low levels of oxygen, and cell extracts of strain ZAS-2 show relatively high levels of NADH oxidase and NADH peroxidase but no catalase activity (Graber and Breznak, 2004). In addition, and quite surprisingly, *T. primitia* encodes a catechol-2,3-dioxygenase (Lucey and Leadbetter, 2014), an enzyme that typically occurs in aerobic bacteria degrading aromatic compounds; it is absent from the other members of the clade. The genomes of *T. primitia* ZAS-2 and *T. azotonutricium* encode homologues of NADH oxidase, but strain RmG30 is the only isolate of termite cluster I (with sequenced genome) that encodes catalase and pyruvate oxidase. It remains to be investigated whether external hemin affects the aerotolerance of strain RmG30, its capacity for fumarate reduction, or its cell yields on glucose.

Taxonomic implications

For the longest time, all members of the phylum '*Spirochaetes*' were classified in a single order (*Spirochaetales*) (Paster, 2015). However, 16S rRNA-based and phylogenomic analyses indicated that the

taxonomic ranks did not appropriately reflect the diversity of the phylum, and numerous taxa have been subsequently elevated to higher ranks (Gupta *et al*., 2013; Yarza *et al*., 2014; Hördt *et al*., 2020). In that course, the family *Treponemataceae* has been reinstated; it currently contains the genera *Treponema* and *Rectinema* (Hördt *et al*., 2020).

However, members of the genus *Treponema* are phylogenetically highly divergent (Norris *et al*., 2015; Paster, 2018). Based on the clear separation of termite cluster I (together with *T. stenostreptum and T. caldarium*) from all other members of the genus *Treponema*, Lilburn *et al*. (1999) already considered it inevitable that 'a new genus or genera will ultimately be created to accommodate spirochaetes of the termite cluster.' This notion is substantiated by the current GTDB taxonomy, which takes into account phylogeny, average nucleotide identity and relative evolutionary distance (Parks *et al*., 2018; Parks *et al*., 2020). The GTDB taxonomy distinguishes two separate, family-level lineages in the order 'Treponematales': (i) *Treponemataceae*, which comprise the majority of all *Treponema* species but distinguishes several genus-level taxa, and (ii) 'Treponemataceae_B', which include *T. caldarium*, strain RmG30, and members of termite cluster I as separate genus-level taxa (Fig. 3). The membership of *T. stenostrepta* and *T. isoptericolens*, whose genomes have not been sequenced, in 'Treponemataceae_B' is highly supported by the 16S rRNA-based phylogeny (Fig. 2).

The nucleotide identities of the genomes and/or the respective 16S rRNA genes (Fig. 4) corroborate that each species in the family 'Treponemataceae_B' represents separate genus-level lineages. This agrees with the considerable phenotypic differences between the species, concerning not only cell shape, flagellar arrangement, genome size and G + C content but also metabolic traits such as substrate and product range, response to oxygen, and the capacity for reductive acetogenesis (Tables 2 and 3).

Based on these results, we describe strain RmG30 as the type strain of *Breznakiella homolactica* gen. nov. sp. nov. and propose classification of all members of the 'Treponemataceae_B' in the new family '*Termitinemataceae*'. The formal description of this family and the reclassification of all *Treponema* spp. in its radiation into separate genera, with '*Termitinema*' [*Treponema primitia*] as type genus, will be addressed in a separate publication. In addition, the taxonomic ranks suggested by GTDB will require further taxonomic acts, such as elevation of the genus *Rectinema* to family level ('*Rectinemataceae*'), and the reclassification of *Trepone mataceae*, *Termitinemataceae* and '*Rectinemataceae*' in the new order '*Treponematales*'.

Description of Breznakiella *gen. nov.*

Etymology: Brez.na.ki.el'la. N. L. dimin. fem. n. *Breznakiella*, named after the American microbiologist John A. Breznak, in recognition of his fundamental contributions to the studies on termite gut treponemes.

The description is as given for *Breznakiella homolactica* sp. nov., which is the type species. The genus is monospecific and has been separated from other members of the family '*Termitinemataceae*' based on physiology and phylogenetic analyses of genome and 16S rRNA gene sequences.

Description of Breznakiella homolactica sp. nov.

Etymology: ho.mo.lac'ti.ca. Gr. adj. *homoios*, the same, similar; N.L. neut. n. *acidum lacticum*, lactic acid; N.L. fem. adj. *homolactica*, referring to a metabolic analogy to other bacteria with homolactic fermentation.

Cells are helical, with a diameter of 0.2 μm, a length of 10–25 μm, and a wavelength of about 1.0 μm. Motile by two periplasmic flagella inserted at opposite ends of the cytoplasmic cylinder. Spherical bodies with a diameter of 2–4 μm are formed in stationary phase cultures. Mesophilic, grows optimally at 35°C (range 20–37°C); no growth at 40°C. Optimum pH for growth is 7.3–7.8 (range 6.5–7.8). Fermentative metabolism. Energy sources include D-glucose, D-mannose, D-galactose, D-fructose, D-xylose, L-arabinose, D-ribose, D-trehalose and *N*-acetylglucosamine. No growth on L-rhamnose, D-mannitol, D-gluconic acid, D-glucuronic acid, D-cellobiose, D-maltose, D-sucrose, D-lactose, starch, cellulose, xylan, pyruvate, lactate, formate, or $H_2 + CO_2$. Lactate is the only product from all sugars tested. Requires yeast extract and Casamino acids. Obligately anaerobic, but resting cells reduce oxygen. Genome size is 4.65 Mbp, G + C content is 52.9 mol.% (based on the type strain).

Source: The intestinal tract of the Madeira cockroach, *Rhyparobia maderae* (Fabricius 1781).

Type strain: strain RmG30 = DSM 111054 = JCM 39135. GenBank accession numbers: MW396710 (16S rRNA gene); CP067089 (genome).

Experimental procedures

Microbiological media

Cultures were routinely grown in medium AM-5, an anoxic, bicarbonate-buffered mineral medium supplemented with vitamins and other growth factors (Tegtmeier *et al*., 2016), which was amended with yeast extract and Casamino acids (0.1% each), cysteine and DTT (1 mM each) as reducing agents, and resazurin

Table 2. Characteristics that differentiate strain RmG30 from other species in the radiation of the new family '*Termitinemataceae*'.

Characteristics	Strain RmG30	*Treponema primitia*[a]	*Treponema azotonutricium*[a]	*Treponema isoptericolens*[b]	*Treponema caldarium*[c]	*Treponema stenostreptum*[d]
Habitat	Cockroach gut	Termite gut	Termite gut	Termite gut	Hot spring sediment	Freshwater sediment
Cell diameter (μm)	0.2	0.2–0.3	0.2–0.3	0.4–0.5	0.2–0.3	0.2–0.3
Cell length (μm)	10–25	3–7	10–12	12–20	15–45	15–45
Wavelength (μm)	1.0	2.3	1.2	6.5	0.6[e]	1.2
Flagellar arrangement	1:2:1	1:2:1	1:2:1	3:6:3	1:2:1	1:2:1
Genome size (Mbp)	4.65	4.06	3.86	NA	3.24	NA
G + C content (mol.%)[f]	52.9	50.8	49.8	47.7[g]	45.6	60.2[h]
pH optimum	7.3–7.8	7.2	ND	7.2–7.4	7.2–7.5	7.0–7.5
Temp. optimum (°C)	35	30	30	30	48–52	35–37
Catalase	+[i]	–	–	–	ND[j]	–
Fermentation products[k]	Lactate	Acetate	Acetate, ethanol, CO_2, H_2	Ethanol, CO_2	Acetate, lactate, CO_2, H_2	Ethanol, acetate, lactate, CO_2, H_2
Growth on $H_2 + CO_2$	–	+	–	–	ND	ND

–, no activity; NA, not available; ND, not determined.
[a]Data from Graber and Breznak (2004), Graber *et al*. (2004), Norris *et al*. (2015).
[b]Data from Dröge *et al*. (2008).
[c]Data from Pohlschroeder *et al*. (1994).
[d]Data from Zuelzer (1912) and Norris *et al*. (2015).
[e]Estimated from Fig. 1 in Pohlschroeder *et al*. (1994).
[f]Based on genome sequences.
[g]Determined by HPLC.
[h]Estimated from buoyant density of DNA in CsCl (Canale-Parola *et al*., 1968).
[i]Expressed only in the presence of hemin.
[j]Not encoded in genome.
[k]Product(s) from glucose (maltose in *T. isoptericolens*), in stoichiometric order.

Table 3. Differences in substrate utilization by strain RmG30 and other species in the new family '*Termitinemataceae*'.

Substrate	Strain RmG30	*Treponema primitia*[a]	*Treponema azotonutricium*[a]	*Treponema isoptericolens*[b]	*Treponema caldarium*[c]	*Treponema stenostreptum*[d]
Glucose	+	+	+	−	+	+
Mannose	+			−	+	
Fructose	+		+	+	+	
Galactose	+			−	+	
Xylose	+	+	+	+	+	
Arabinose	+	+	−	+	+	
Ribose	+	−	+	−	−	
Mannitol	−	+	−		−	
Maltose	−	+	+	+	+	
Cellobiose	−	+	+	+	+	
Trehalose	+		−	+		
Sucrose	−		−	−	+	
Lactose	−				+	
Starch	−				+	

+, utilized; −, not utilized.
[a]Data from Graber and Breznak (2004) and Graber *et al*. (2004).
[b]Data from Dröge *et al*. (2008).
[c]Data from Pohlschroeder *et al*. (1994).
[d]Data from Zuelzer (1912) and Norris *et al*. (2015).

(0.8 mg L^{-1}) as redox indicator. Non-reduced anoxic medium received cystine (0.5 mM) from an acidic stock solution (250 mM in 1 M HCl) as sulfur source. Unless otherwise indicated, this 'basal medium' was amended with glucose (8 mM), dispensed (5 ml) into 16-ml rubber-stoppered culture tubes, gassed with a headspace of N_2/CO_2, and inoculated with a fresh preculture (0.1 ml).

To assess the pH range of growth, the initial pH of the medium was adjusted by varying the mixing ratio of N_2 and CO_2 in the headspace gas; Widdel and Bak, 1992). The N_2/CO_2 ratio routinely used during isolation and initial experiments was 80:20 (vol./vol.), resulting in a medium pH of 7.0. It was changed to 90:10 (vol./vol.), resulting in a medium pH of 7.3, after we realized that

strain RmG30 grew better if the medium was slightly alkaline. For growth tests at pH 8.5, bicarbonate buffer was replaced with *N*-tris(hydroxymethyl)methyl-3-aminopropanesulfonic acid at a final concentration of 20 mM, and N_2 was the headspace gas.

Enrichment and isolation

Rhyparobia maderae was obtained from a commercial breeder (Jörg Bernhardt, Helbigsdorf, Germany; http://www.schaben-spinnen.de) and maintained as previously described (Schauer *et al*., 2012). An adult female cockroach was dissected, and the whole gut was placed in a culture tube containing 2-mm glass beads (2 g). After addition of 5 ml basal medium, the tube was closed with a rubber stopper, the headspace was gassed with N_2/CO_2 (80:20, vol./vol.), and the gut was homogenized by vortexing for 2 min. The gut homogenate was passed through a cellulose ester membrane filter (Merck Millipore) with pore diameter of 0.3 μm, and the filtrate was serially diluted in deep-agar tubes containing basal medium with 1% agar under an N_2/CO_2 headspace. The pure culture was isolated by picking single colonies from the ultimate dilution step that showed growth.

Growth and physiology

Growth was measured photometrically by following the increase in optical density at 578 nm (OD_{578}) using a culture tube photometer (Spectronic 20^+, Milton Roy; path length 1.3 cm). Dry weight was determined with replicate cultures grown on glucose (8 mM) in 1-L glass vessels containing 500 ml basal medium. After OD measurement, the cells were harvested by centrifugation (10 000*g*; 20 min), washed with ammonium acetate solution (20 mM), and dried at 60°C until weight constancy.

Growth on other substrates was tested in basal medium supplemented with the respective substrates (8 mM, except 4 mM for disaccharides); carboxylic acids were supplied as sodium salts. Polysaccharides (6 mg ml^{-1}) were autoclaved in the tubes before basal medium was added. Growth on H_2 + CO_2 was tested by adding 5 ml H_2 to the headspace of culture tubes with (bicarbonate-buffered) basal medium. Fumarate reduction was tested by adding 16 mM fumarate to basal medium with glucose, sodium formate, or H_2.

Oxygen tolerance was tested in culture tubes with non-reduced basal medium with 8 mM glucose under N_2/CO_2, which received different volumes of air in the headspace and were incubated on a roller mixer (60 rpm). The effect of oxygen on glucose turnover was tested with washed cell suspensions. Cells were grown on the same medium (100 ml) in rubber-stopped, centrifugable glass bottles (150 ml) under N_2/CO_2, harvested in the exponential growth phase by centrifugation (3000*g*; 30 min) and resuspended in 10 ml anoxic buffer (30 mM $NaHCO_3$, 40 mM NaCl, pH 7.0) under N_2/CO_2. The cell suspensions (0.3 mg ml^{-1}) were amended with 8 mM glucose and divided into two cohorts: one was supplemented with 1 mM DTT and was incubated under anoxic conditions, the other was supplemented with air at a headspace concentration of 0.4% O_2 to create microoxic conditions. The cell suspensions were incubated on a shaker (100 rpm) at 30°C; O_2 concentration was monitored with a Fibox 4 trace meter and SP-PSt6-NAU sensor spots (PreSens; https://www.presens.de/) and maintained between 0.2% and 0.4% throughout the incubation period by adding defined volumes of air at regular intervals.

Oxidase activity was tested with glucose-grown cultures in basal medium using oxidase test strips (Bactident, Merck, Darmstadt, Germany); *Bacillus subtilis* (oxidase-positive) and *Escherichia coli* (oxidase-negative) were used as controls. Catalase activity was tested by checking the formation of gas bubbles after adding a drop of H_2O_2 (3%) to cell pellets of glucose-grown cultures; *E. coli* (catalase-positive) and *Elusimicrobium minutum* (catalase-negative; Geissinger *et al*., 2009) were used as controls. The effect of hemin on catalase expression was tested by adding hemin (2 μg ml^{-1}; Sigma-Aldrich) from a stock solution (5 mg ml^{-1} in 50 mM NaOH). To avoid false-positive reactions, the suspended cells were separated from precipitated hemin before centrifugation and washed twice with phosphate-buffered saline (10 mM Na_2HPO_4, 1.8 mM KH_2PO_4, 137 mM NaCl, 2.7 mM KCl, pH 7.2).

Metabolic products

Hydrogen was analysed in the culture headspace by gas chromatography, using a molecular sieve column and a thermal conductivity detector (Schuler and Conrad, 1990). Other fermentation products were analysed in the culture supernatant by high-performance liquid chromatography after centrifugation at 10 000*g* for 10 min and acidification with H_2SO_4 to 50 mM final concentration, using a system equipped with an ion-exclusion column and a refractive index detector (Schauer *et al*., 2012). For the calculation of electron recoveries, all metabolites were formally oxidized to CO_2, and the number of valence electrons theoretically released during product formation was compared with that of the dissimilated substrate (Tholen *et al*., 1997).

Light and electron microscopy

Cultures were examined by light microscopy using an Axiophot photomicroscope (Zeiss, Oberkochen,

Germany). Non-stained cultures were routinely examined using phase-contrast illumination (100× objective).

For electron microscopy, cells were fixed with glutaraldehyde and postfixed with osmium tetroxide before dehydrating in a graded series of ethanol and embedding in Spurr's resin (Zheng *et al*., 2016). Alternatively, 2-μl samples of concentrated cell suspensions were high-pressure frozen, freeze-substituted with HUGA (0.5% uranyl acetate, 0.5% glutaraldehyde, 5% H_2O in acetone), and embedded in Epon 812 substitute resin, as previously described (Renicke *et al*., 2017). Ultrathin sections were cut with a microtome equipped with a diamond knife and contrasted with uranyl acetate and lead citrate. The sections were examined with a Philips EM 208 transmission electron microscope.

Genome sequencing and annotation

Genomic DNA was prepared using cetyltrimethylammonium bromide extraction (Winnepenninckx *et al*., 1993) and commercially sequenced (GATC-Eurofins, Konstanz, Germany) on a PacBio RS platform using one SMRT cell (insert size up to 10 kbp). Reads were assembled with the PacBio SMRT Portal software (version 2.3.0) using the Hierarchical Genome Assembly Process for assembly and Quiver for polishing (Chin *et al*., 2013). The polished single contig was circularized with Circlator (Hunt *et al*., 2015).

The genome sequence of strain RmG30 has been submitted to GenBank (https://www.ncbi.nlm.nih.gov; accession number CP067089; circularized) and to the Integrated Microbial Genomes and Microbiomes database (IMG/M) of the Joint Genome Institute (JGI) (https://img.jgi.doe.gov; taxon ID 2772190975; not circularized). The genome was annotated via the IMG annotation pipeline (v.4.16.1; Chen *et al*., 2019). For the analysis of the metabolic pathways, annotation results were verified, and missing functions were identified using Blast with a threshold *E*-value of 1E–5. Hydrogenases were classified using the HydDB reference database (https://services.birc.au.dk/hyddb/; Søndergaard *et al*., 2016).

Phylogenetic analyses

The 16S rRNA gene of strain RmG30 was amplified with *Bacteria*-specific primers and sequenced by Sanger sequencing as previously described (Strassert *et al*., 2010); the sequence has been submitted to GenBank (ID: MW396710). The sequence was aligned with the SINA aligner (Pruesse *et al*., 2012) and imported into the reference alignment of the Silva database (version 132; Pruesse *et al*., 2007); additional sequences were downloaded from GenBank. The alignments were manually curated using the ARB software package (version 6.0.6; Ludwig *et al*., 2004). A maximum-likelihood tree of the 16S rRNA genes was inferred from 1275 unambiguous aligned positions (sites with more than 50% gaps were masked) using the PhyML algorithm (version 3.3; Guindon *et al*., 2010) with GTR model and aBayes branch supports (Anisimova *et al*., 2011) included in ARB. Pairwise sequence identities of 16S rRNA genes are based on a distance matrix of the unfiltered alignment generated in ARB.

The genomes of strain RmG30 and other members of termite cluster I were phylogenetically classified within the taxonomic framework of the Genome Taxonomy Database (GTDB, release 89) using the GTDB toolkit (GTDB-tk, version 1.3.0; Chaumeil *et al*., 2020). A maximum-likelihood tree based on the genomes was inferred from a concatenated alignment of 120 bacterial single-copy genes (5040 amino acid positions) using the PhyML algorithm with LG model and aBayes branch supports. The average nucleotide identities of the genomes were calculated with FastANI (version 1.3; Jain *et al*., 2018).

Acknowledgements

This study was funded by the Deutsche Forschungsgemeinschaft (DFG) in the collaborative research center SFB 987 (Microbial Diversity in Environmental Signal Response) and by the Max Planck Society (MPG). Yulin Song was supported by a fellowship of the China Scholarship Council (CSC). We thank Karen A. Brune for linguistic comments on the manuscript.

References

Abt, B., Göker, M., Scheuner, C., Han, C., Lu, M., Misra, M., *et al*. (2013) Genome sequence of the thermophilic freshwater bacterium *Spirochaeta caldaria* type strain ($H1^T$), reclassification of *Spirochaeta caldaria*, *Spirochaeta stenostrepta*, and *Spirochaeta zuelzerae* in the genus *Treponema* as *Treponema caldaria* comb. nov., *Treponema stenostrepta* comb. nov., and *Treponema zuelzerae* comb. nov., and emendation of the genus *Treponema*. *Stand Genomic Sci* **8**: 88–105.

Allen, K.D., Miller, D.V., Rauch, B.J., Perona, J.J., and White, R.H. (2015) Homocysteine is biosynthesized from aspartate semialdehyde and hydrogen sulfide in methanogenic archaea. *Biochemistry* **54**: 3129–3132.

Anisimova, M., Gil, M., Dufayard, J.F., Dessimoz, C., and Gascuel, O. (2011) Survey of branch support methods demonstrates accuracy, power, and robustness of fast likelihood-based approximation schemes. *Syst Biol* **60**: 685–699.

Bauer, E., Lampert, N., Mikaelyan, A., Köhler, T., Maekawa, K., and Brune, A. (2015) Physicochemical conditions, metabolites and community structure of the bacterial microbiota in the gut of wood-feeding cockroaches (Blaberidae: Panesthiinae). *FEMS Microbiol Ecol* **91**: 1–14.

Bauer, S., Tholen, A., Overmann, J., and Brune, A. (2000) Characterization of abundance and diversity of lactic acid bacteria in the hindgut of wood- and soil-feeding termites

by molecular and culture-dependent techniques. *Arch Microbiol* **173**: 126–137.
Baureder, M., and Hederstedt, L. (2013) Heme proteins in lactic acid bacteria. *Adv Microb Physiol* **62**: 1–43.
Berchtold, M., Ludwig, W., and König, H. (1994) 16S rDNA sequence and phylogenetic position of an uncultivated spirochete from the hindgut of the termite *Mastotermes darwiniensis* Froggatt. *FEMS Microbiol Lett* **123**: 269–273.
Berlanga, M., Llorens, C., Comas, J., and Guerrero, R. (2016) Gut bacterial community of the xylophagous cockroaches *Cryptocercus punctulatus* and *Parasphaeria boleiriana*. *PLoS One* **11**: e0152400.
Bourguignon, T., Lo, N., Cameron, S.L., Šobotník, J., Hayashi, Y., Shigenobu, S., *et al*. (2015) The evolutionary history of termites as inferred from 66 mitochondrial genomes. *Mol Biol Evol* **32**: 406–421.
Bourguignon, T., Lo, N., Dietrich, C., Šobotník, J., Sidek, S., Roisin, Y., *et al*. (2018) Rampant host switching shaped the termite gut microbiome. *Curr Biol* **28**: 649–654.
Breznak, J.A. (2002) Phylogenetic diversity and physiology of termite gut spirochetes. *Integr Comp Biol* **42**: 313–318.
Breznak, J.A., and Leadbetter, J.R. (2006) Termite gut spirochetes. In *The Prokaryotes*, 3rd ed, Vol. **7**, Dworkin, M., Falkow, S., Rosenberg, E., Schleifer, K.-H., and Stackebrandt, E. (eds). New York: Springer, pp. 318–329.
Brioukhanov, A.L., and Netrusov, A.I. (2007) Aerotolerance of strictly anaerobic microorganisms and factors of defense against oxidative stress: a review. *Appl Biochem Microbiol* **43**: 567–582.
Brioukhanov, A.L., and Netrusov, A.I. (2012) The positive effect of exogenous hemin on a resistance of strict anaerobic archaeon *Methanobrevibacter arboriphilus* to oxidative stresses. *Curr Microbiol* **65**: 375–383.
Brune, A. (2014) Symbiotic digestion of lignocellulose in termite guts. *Nat Rev Microbiol* **12**: 168–180.
Brune, A., and Dietrich, C. (2015) The gut microbiota of termites: digesting the diversity in the light of ecology and evolution. *Annu Rev Microbiol* **69**: 145–166.
Canale-Parola, E., Udris, Z., and Mandel, M. (1968) The classification of free-living spirochetes. *Arch Mikrobiol* **63**: 385–397.
Chaumeil, P.A., Mussig, A.J., Hugenholtz, P., and Parks, D. H. (2020) GTDB-Tk: a toolkit to classify genomes with the Genome Taxonomy Database. *Bioinformatics* **36**: 1925–1927.
Chen, I.A., Chu, K., Palaniappan, K., Pillay, M., Ratner, A., Huang, J., *et al*. (2019) IMG/M v.5.0: an integrated data management and comparative analysis system for microbial genomes and microbiomes. *Nucleic Acids Res* **47**: D666–D677.
Chin, C.S., Alexander, D.H., Marks, P., Klammer, A.A., Drake, J., Heiner, C., *et al*. (2013) Nonhybrid, finished microbial genome assemblies from long-read SMRT sequencing data. *Nat Methods* **10**: 563–569.
Chouvenc, T., Šobotník, J., Engel, M.S., and Bourguignon, T. (2021) Termite evolution: mutualistic associations, key innovations, and the rise of Termitidae. *Cell Mol Life Sci* **78**: 2749–2769.
Condon, S. (1987) Responses of lactic-acid bacteria to oxygen. *FEMS Microbiol Lett* **46**: 269–280.
Dietrich, C., Köhler, T., and Brune, A. (2014) The cockroach origin of the termite gut microbiota: patterns in bacterial community structure reflect major evolutionary events. *Appl Environ Microbiol* **80**: 2261–2269.
Djernæs, M., Varadínová, Z.K., Kotyk, M., Eulitz, U., and Klass, K.D. (2020) Phylogeny and life history evolution of Blaberoidea (Blattodea). *Arthropod Syst Phyl* **78**: 29–67.
Drake, H.L. (1994) Acetogenesis, acetogenic bacteria, and the acetyl-CoA "wood/Ljungdahl" pathway: past and current perspectives. In *Acetogenesis*, Drake, H.L. (ed). Boston: Springer, pp. 3–60.
Dröge, S., Rachel, R., Radek, R., and König, H. (2008) *Treponema isoptericolens* sp. nov., a novel spirochaete from the hindgut of the termite *Incisitermes tabogae*. *Int J Syst Evol Microbiol* **58**: 1079–1083.
Engesser, D.M., and Hammes, W.P. (1994) Non-heme catalase activity of lactic-acid bacteria. *Syst Appl Microbiol* **17**: 11–19.
Geissinger, O., Herlemann, D.P., Mörschel, E., Maier, U.G., and Brune, A. (2009) The ultramicrobacterium "*Elusimicrobium minutum*" gen. nov., sp. nov., the first cultivated representative of the termite group 1 phylum. *Appl Environ Microbiol* **75**: 2831–2840.
Ghebreamlak, S.M., and Mansoorabadi, S.O. (2020) Divergent members of the nitrogenase superfamily: tetrapyrrole biosynthesis and beyond. *ChemBioChem* **21**: 1723–1728.
Graber, J.R., and Breznak, J.A. (2004) Physiology and nutrition of *Treponema primitia*, an H_2/CO_2-acetogenic spirochete from termite hindguts. *Appl Environ Microbiol* **70**: 1307–1314.
Graber, J.R., and Breznak, J.A. (2005) Folate cross-feeding supports symbiotic homoacetogenic spirochetes. *Appl Environ Microbiol* **71**: 1883–1889.
Graber, J.R., Leadbetter, J.R., and Breznak, J.A. (2004) Description of *Treponema azotonutricium* sp. nov. and *Treponema primitia* sp. nov., the first spirochetes isolated from termite guts. *Appl Environ Microbiol* **70**: 1315–1320.
Guindon, S., Dufayard, J.F., Lefort, V., Anisimova, M., Hordijk, W., and Gascuel, O. (2010) New algorithms and methods to estimate maximum-likelihood phylogenies: assessing the performance of PhyML 3.0. *Syst Biol* **59**: 307–321.
Gupta, R.S., Mahmood, S., and Adeolu, M. (2013) A phylogenomic and molecular signature based approach for characterization of the phylum *Spirochaetes* and its major clades: proposal for a taxonomic revision of the phylum. *Front Microbiol* **4**: 217.
Hervé, V., Liu, P., Dietrich, C., Sillam-Dussès, D., Stiblik, P., Šobotník, J., and Brune, A. (2020) Phylogenomic analysis of 589 metagenome-assembled genomes encompassing all major prokaryotic lineages from the gut of higher termites. *PeerJ* **8**: e8614.
Hongoh, Y., Ekpornprasit, L., Inoue, T., Moriya, S., Trakulnaleamsai, S., Ohkuma, M., *et al*. (2006) Intracolony variation of bacterial gut microbiota among castes and ages in the fungus-growing termite *Macrotermes gilvus*. *Mol Ecol* **15**: 505–516.
Hördt, A., López, M.G., Meier-Kolthoff, J.P., Schleuning, M., Weinhold, L.M., Tindall, B.J., *et al*. (2020) Analysis of 1,000+ type-strain genomes substantially improves taxonomic classification of *Alphaproteobacteria*. *Front Microbiol* **11**: 468.

Hunt, M., Silva, N.D., Otto, T.D., Parkhill, J., Keane, J. A., and Harris, S.R. (2015). Circlator: automated circularization of genome assemblies using long sequencing reads. *Genome Biol*, **16**, 1–10.

Iida, T., Ohkuma, M., Ohtoko, K., and Kudo, T. (2000) Symbiotic spirochetes in the termite hindgut: phylogenetic identification of ectosymbiotic spirochetes of oxymonad protists. *FEMS Microbiol Ecol* **34**: 17–26.

Ikeda-Ohtsubo, W., Strassert, J.F., Köhler, T., Mikaelyan, A., Gregor, I., McHardy, A.C., *et al*. (2016) '*Candidatus* Adiutrix intracellularis', an endosymbiont of termite gut flagellates, is the first representative of a deep-branching clade of *Deltaproteobacteria* and a putative homoacetogen. *Environ Microbiol* **18**: 2548–2564.

Imlay, J.A. (2019) Where in the world do bacteria experience oxidative stress? *Environ Microbiol* **21**: 521–530.

Jain, C., Rodriguez, R.L., Phillippy, A.M., Konstantinidis, K. T., and Aluru, S. (2018) High throughput ANI analysis of 90K prokaryotic genomes reveals clear species boundaries. *Nat Commun* **9**: 5114.

Kandler, O. (1983) Carbohydrate metabolism in lactic acid bacteria. *Antonie Van Leeuwenhoek* **49**: 209–224.

Lampert, N., Mikaelyan, A., and Brune, A. (2019) Diet is not the primary driver of bacterial community structure in the gut of litter-feeding cockroaches. *BMC Microbiol* **19**: 1–14.

Leadbetter, J.R., Schmidt, T.M., Graber, J.R., and Breznak, J.A. (1999) Acetogenesis from H_2 plus CO_2 by spirochetes from termite guts. *Science* **283**: 686–689.

Leidy, J. (1881) The parasites of the termites. *J Acad Nat Sci Philadelphia, 2nd series* **8**: 425–447.

Lilburn, T.G., Kim, K.S., Ostrom, N.E., Byzek, K.R., Leadbetter, J.R., and Breznak, J.A. (2001) Nitrogen fixation by symbiotic and free-living spirochetes. *Science* **292**: 2495–2498.

Lilburn, T.G., Schmidt, T.M., and Breznak, J.A. (1999) Phylogenetic diversity of termite gut spirochaetes. *Environ Microbiol* **1**: 331–345.

Lucey, K.S., and Leadbetter, J.R. (2014) Catechol 2,3-dioxygenase and other *meta*-cleavage catabolic pathway genes in the 'anaerobic' termite gut spirochete *Treponema primitia*. *Mol Ecol* **23**: 1531–1543.

Ludwig, W., Strunk, O., Westram, R., Richter, L., Meier, H., and Yadhukumar, S. (2004) ARB: a software environment for sequence data. *Nucleic Acids Res* **32**: 1363–1371.

Matson, E.G., Gora, K.G., and Leadbetter, J.R. (2011) Anaerobic carbon monoxide dehydrogenase diversity in the homoacetogenic hindgut microbial communities of lower termites and the wood roach. *PLoS One* **6**: e19316.

Mayberry, W.R., Prochazka, G.J., and Payne, W.J. (1968) Factors derived from studies of aerobic growth in minimal media. *J Bacteriol* **96**: 1424–1426.

McCoy, A.J., Adams, N.E., Hudson, A.O., Gilvarg, C., Leustek, T., and Maurelli, A.T. (2006) L,L-diaminopimelate aminotransferase, a trans-kingdom enzyme shared by chlamydia and plants for synthesis of diaminopimelate/lysine. *Proc Natl Acad Sci U S A* **103**: 17909–17914.

Mikaelyan, A., Dietrich, C., Köhler, T., Poulsen, M., Sillam-Dussès, D., and Brune, A. (2015a) Diet is the primary determinant of bacterial community structure in the guts of higher termites. *Mol Ecol* **24**: 5284–5295.

Mikaelyan, A., Köhler, T., Lampert, N., Rohland, J., Boga, H., Meuser, K., and Brune, A. (2015b) Classifying the bacterial gut microbiota of termites and cockroaches: a curated phylogenetic reference database (DictDb). *Syst Appl Microbiol* **38**: 472–482.

Nakahigashi, K., Toya, Y., Ishii, N., Soga, T., Hasegawa, M., Watanabe, H., *et al*. (2009) Systematic phenome analysis of *Escherichia coli* multiple-knockout mutants reveals hidden reactions in central carbon metabolism. *Mol Syst Biol* **5**: 306.

Noda, S., Ohkuma, M., Yamada, A., Hongoh, Y., and Kudo, T. (2003) Phylogenetic position and in situ identification of ectosymbiotic spirochetes on protists in the termite gut. *Appl Environ Microbiol* **69**: 625–633.

Noda, S., Shimizu, D., Yuki, M., Kitade, O., and Ohkuma, M. (2018) Host-symbiont cospeciation of termite-gut cellulolytic protists of the genera *Teranympha* and *Eucomonympha* and their *Treponema* endosymbionts. *Microbes Environ* **33**: 26–33.

Norris, S.J., Paster, B.J., and Smibert, R.M. (2015) *Treponema*. In *Bergey's Manual of Systematics of Archaea and Bacteria*, Trujillo, M.E., Dedysh, S., DeVos, P., Hedlund, B., Kämpfer, P., Rainey, F.A., and Whitman, W.B. (eds). Wiley Online Library. https://doi.org/10.1002/9781118960608.gbm01249.

Ohkuma, M., and Brune, A. (2011) Diversity, structure, and evolution of the termite gut microbial community. In *Biology of Termites: A Modern Synthesis*, Bignell, D., Roisin, Y., and Lo, N. (eds). Dordrecht: Springer, pp. 413–438.

Ohkuma, M., Iida, T., and Kudo, T. (1999) Phylogenetic relationships of symbiotic spirochetes in the gut of diverse termites. *FEMS Microbiol Lett* **181**: 123–129.

Ohkuma, M., and Kudo, T. (1996) Phylogenetic diversity of the intestinal bacterial community in the termite *Reticulitermes speratus*. *Appl Environ Microbiol* **62**: 461–468.

Ohkuma, M., Noda, S., Hattori, S., Iida, T., Yuki, M., Starns, D., *et al*. (2015) Acetogenesis from H_2 plus CO_2 and nitrogen fixation by an endosymbiotic spirochete of a termite-gut cellulolytic protist. *Proc Natl Acad Sci U S A* **112**: 10224–10230.

Okano, K., Yoshida, S., Tanaka, T., Ogino, C., Fukuda, H., and Kondo, A. (2009) Homo-D-lactic acid fermentation from arabinose by redirection of the phosphoketolase pathway to the pentose phosphate pathway in L-lactate dehydrogenase gene-deficient *Lactobacillus plantarum*. *Appl Environ Microbiol* **75**: 5175–5178.

Otani, S., Mikaelyan, A., Nobre, T., Hansen, L.H., Kone, N. A., Sorensen, S.J., *et al*. (2014) Identifying the core microbial community in the gut of fungus-growing termites. *Mol Ecol* **23**: 4631–4644.

Ottesen, E.A., and Leadbetter, J.R. (2010) Diversity of formyltetrahydrofolate synthetases in the guts of the wood-feeding cockroach *Cryptocercus punctulatus* and the omnivorous cockroach *Periplaneta americana*. *Appl Environ Microbiol* **76**: 4909–4913.

Ottesen, E.A., and Leadbetter, J.R. (2011) Formyltetrahydrofolate synthetase gene diversity in the guts

of higher termites with different diets and lifestyles. *Appl Environ Microbiol* **77**: 3461–3467.
Parks, D.H., Chuvochina, M., Chaumeil, P.A., Rinke, C., Mussig, A.J., and Hugenholtz, P. (2020) A complete domain-to-species taxonomy for bacteria and archaea. *Nat Biotechnol* **38**: 1079–1086.
Parks, D.H., Chuvochina, M., Waite, D.W., Rinke, C., Skarshewski, A., Chaumeil, P.A., and Hugenholtz, P. (2018) A standardized bacterial taxonomy based on genome phylogeny substantially revises the tree of life. *Nat Biotechnol* **36**: 996–1004.
Parks, D.H., Rinke, C., Chuvochina, M., Chaumeil, P.A., Woodcroft, B.J., Evans, P.N., *et al*. (2017) Recovery of nearly 8,000 metagenome-assembled genomes substantially expands the tree of life. *Nat Microbiol* **2**: 1533–1542.
Paster, B.J. (2015) *Spirochaetes*. In *Bergey's Manual of Systematics of Archaea and Bacteria*, Trujillo, M.E., Dedysh, S., DeVos, P., Hedlund, B., Kämpfer, P., Rainey, F.A., and Whitman, W.B. (eds). Wiley Online Library. https://doi.org/10.1002/9781118960608.pbm00023.
Paster, B.J. (2018) Other organisms. Hindgut spirochetes of termites and cockroaches. In *Bergey's Manual of Systematics of Archaea and Bacteria*, Trujillo, M.E., Dedysh, S., DeVos, P., Hedlund, B., Kämpfer, P., Rainey, F.A., and Whitman, W.B. (eds). Wiley Online Library. https://doi.org/10.1002/9781118960608.fbm00242.pub2.
Paster, B.J., Dewhirst, F.E., Cooke, S.M., Fussing, V., Poulsen, L.K., and Breznak, J.A. (1996) Phylogeny of not-yet-cultured spirochetes from termite guts. *Appl Environ Microbiol* **62**: 347–352.
Pester, M., and Brune, A. (2006) Expression profiles of fhs (FTHFS) genes support the hypothesis that spirochaetes dominate reductive acetogenesis in the hindgut of lower termites. *Environ Microbiol* **8**: 1261–1270.
Plumbridge, J., and Vimr, E. (1999) Convergent pathways for utilization of the amino sugars *N*-acetylglucosamine, *N*-acetylmannosamine, and *N*-acetylneuraminic acid by *Escherichia coli*. *J Bacteriol* **181**: 47–54.
Pohlschroeder, M., Leschine, S.B., and Canaleparola, E. (1994) *Spirochaeta caldaria* sp. nov., a thermophilic bacterium that enhances cellulose degradation by *Clostridium thermocellum*. *Arch Microbiol* **161**: 17–24.
Pruesse, E., Peplies, J., and Glöckner, F.O. (2012) SINA: accurate high-throughput multiple sequence alignment of ribosomal RNA genes. *Bioinformatics* **28**: 1823–1829.
Pruesse, E., Quast, C., Knittel, K., Fuchs, B.M., Ludwig, W., Peplies, J., and Glöckner, F.O. (2007) SILVA: a comprehensive online resource for quality checked and aligned ribosomal RNA sequence data compatible with ARB. *Nucleic Acids Res* **35**: 7188–7196.
Renicke, C., Allmann, A.K., Lutz, A.P., Heimerl, T., and Taxis, C. (2017) The mitotic exit network regulates spindle pole body selection during sporulation of *Saccharomyces cerevisiae*. *Genetics* **206**: 919–937.
Rosenthal, A.Z., Matson, E.G., Eldar, A., and Leadbetter, J. R. (2011) RNA-seq reveals cooperative metabolic interactions between two termite-gut spirochete species in co-culture. *ISME J* **5**: 1133–1142.
Rosenthal, A.Z., Zhang, X., Lucey, K.S., Ottesen, E.A., Trivedi, V., Choi, H.M., *et al*. (2013) Localizing transcripts to single cells suggests an important role of uncultured deltaproteobacteria in the termite gut hydrogen economy. *Proc Natl Acad Sci U S A* **110**: 16163–16168.
Sah, S., Aluri, S., Rex, K., and Varshney, U. (2015) One-carbon metabolic pathway rewiring in *Escherichia coli* reveals an evolutionary advantage of 10-formyltetrahydrofolate synthetase (Fhs) in survival under hypoxia. *J Bacteriol* **197**: 717–726.
Salmassi, T.M., and Leadbetter, J.R. (2003) Analysis of genes of tetrahydrofolate-dependent metabolism from cultivated spirochaetes and the gut community of the termite *Zootermopsis angusticollis*. *Microbiology* **149**: 2529–2537.
Schauer, C., Thompson, C., and Brune, A. (2014) Pyrotag sequencing of the gut microbiota of the cockroach *Shelfordella lateralis* reveals a highly dynamic core but only limited effects of diet on community structure. *PLoS One* **9**: e85861.
Schauer, C., Thompson, C.L., and Brune, A. (2012) The bacterial community in the gut of the cockroach *Shelfordella lateralis* reflects the close evolutionary relatedness of cockroaches and termites. *Appl Environ Microbiol* **78**: 2758–2767.
Schuchmann, K., and Müller, V. (2014) Autotrophy at the thermodynamic limit of life: a model for energy conservation in acetogenic bacteria. *Nat Rev Microbiol* **12**: 809–821.
Schuler, S., and Conrad, R. (1990) Soils contain two different activities for oxidation of hydrogen. *FEMS Microbiol Ecol* **6**: 77–83.
Sokolovskaya, O.M., Shelton, A.N., and Taga, M.E. (2020) Sharing vitamins: Cobamides unveil microbial interactions. *Science* **369**: 6499.
Søndergaard, D., Pedersen, C.N., and Greening, C. (2016) HydDB: a web tool for hydrogenase classification and analysis. *Sci Rep* **6**: 34212.
Strassert, J.F., Desai, M.S., Radek, R., and Brune, A. (2010) Identification and localization of the multiple bacterial symbionts of the termite gut flagellate *Joenia annectens*. *Microbiology* **156**: 2068–2079.
Tai, V., James, E.R., Nalepa, C.A., Scheffrahn, R.H., Perlman, S.J., and Keeling, P.J. (2015) The role of host phylogeny varies in shaping microbial diversity in the hindguts of lower termites. *Appl Environ Microbiol* **81**: 1059–1070.
Tarraran, L., and Mazzoli, R. (2018). Alternative strategies for lignocellulose fermentation through lactic acid bacteria: the state of the art and perspectives. *FEMS Microbiol Lett*, **365**, fny126.
Tegtmeier, D., Riese, C., Geissinger, O., Radek, R., and Brune, A. (2016) *Breznakia blatticola* gen. nov. sp. nov. and *Breznakia pachnodae* sp. nov., two fermenting bacteria isolated from insect guts, and emended description of the family *Erysipelotrichaceae*. *Syst Appl Microbiol* **39**: 319–329.
Tholen, A., Schink, B., and Brune, A. (1997) The gut microflora of *Reticulitermes flavipes*, its relation to oxygen, and evidence for oxygen-dependent acetogenesis by the most abundant *Enterococcus* sp. *FEMS Microbiol Ecol* **24**: 137–149.
Tokuda, G., Mikaelyan, A., Fukui, C., Matsuura, Y., Watanabe, H., Fujishima, M., and Brune, A. (2018) Fiber-

associated spirochetes are major agents of hemicellulose degradation in the hindgut of wood-feeding higher termites. *Proc Natl Acad Sci U S A* **115**: 11996–12004.

Utami, Y.D., Kuwahara, H., Igai, K., Murakami, T., Sugaya, K., Morikawa, T., *et al*. (2019) Genome analyses of uncultured TG2/ZB3 bacteria in 'Margulisbacteria' specifically attached to ectosymbiotic spirochetes of protists in the termite gut. *ISME J* **13**: 455–467.

Warnecke, F., Luginbuhl, P., Ivanova, N., Ghassemian, M., Richardson, T.H., Stege, J.T., *et al*. (2007) Metagenomic and functional analysis of hindgut microbiota of a wood-feeding higher termite. *Nature* **450**: 560–565.

Whittenbury, R. (1960) Two types of catalase-like activity in lactic acid bacteria. *Nature* **187**: 433–434.

Widdel, F., and Bak, F. (1992) Gram-negative mesophilic sulfate-reducing bacteria. In *The Prokaryotes*, Balows, A., Trüper, H.G., Dworkin, M., Harder, W., and Schleifer, K.H. (eds). New York: Springer, pp. 3352–3378.

Winnepenninckx, B., Backeljau, T., and De Wachter, R. (1993) Extraction of high molecular weight DNA from molluscs. *Trends Genet* **9**: 407.

Yarza, P., Yilmaz, P., Pruesse, E., Glöckner, F.O., Ludwig, W., Schleifer, K.H., *et al*. (2014) Uniting the classification of cultured and uncultured bacteria and archaea using 16S rRNA gene sequences. *Nat Rev Microbiol* **12**: 635–645.

Zhang, X., and Leadbetter, J.R. (2012) Evidence for cascades of perturbation and adaptation in the metabolic genes of higher termite gut symbionts. *mBio* **3**: e00223-12.

Zhang, X., Matson, E.G., and Leadbetter, J.R. (2011) Genes for selenium dependent and independent formate dehydrogenase in the gut microbial communities of three lower, wood-feeding termites and a wood-feeding roach. *Environ Microbiol* **13**: 307–323.

Zheng, H., Dietrich, C., Radek, R., and Brune, A. (2016) *Endomicrobium proavitum*, the first isolate of *Endomicrobia* class. nov. (phylum *Elusimicrobia*) – an ultramicrobacterium with an unusual cell cycle that fixes nitrogen with a group IV nitrogenase. *Environ Microbiol* **18**: 191–204.

Zhuang, W.Q., Yi, S., Bill, M., Brisson, V.L., Feng, X., Men, Y., *et al*. (2014) Incomplete wood–Ljungdahl pathway facilitates one-carbon metabolism in organohalide-respiring *Dehalococcoides mccartyi*. *Proc Natl Acad Sci U S A* **111**: 6419–6424.

Zuelzer, M. (1912) Über *Spirochaeta plicatilis* Ehrenberg und deren Verwandtschaftsbeziehungen. *Arch Protistenkd* **24**: 1–59.

Supporting Information

Additional Supporting Information may be found in the online version of this article at the publisher's web-site:

Fig. S1. Expanded version of the phylogenomic tree in the manuscript (Fig. 3), illustrating the relationship of strain RmG30 (red) and other members of the proposed '*Termitinemataceae*' to other lineages in the *Spirochaetales*. Type species of current genera are marked in bold. The tree was rooted using other lineages of *Spirochaetia* as outgroup. Genome sequences were downloaded from GenBank (accession numbers are given), except for strain NkOx-clu11 (Utami *et al*., 2019) and the genomes in UBA8932 (Dong *et al*., 2018), which were provided by the authors.

Fig. S2. The pathways for lysine and methionine biosynthesis in the genome of strain RmG30. Missing genes and the respective reactions are shown in grey. Gene abbreviations and the encoded functions: *asd*, aspartate-semialdehyde dehydrogenase; *ast*, L-aspartate semialdehyde sulfurtransferase; *dapA*, 4-hydroxy-tetrahydrodipicolinate synthase; *dapB*, dihydrodipicolinate reductase; *dapC*, succinyl-diaminopimelate aminotransferase; *dapD*, tetrahydrodipicolinate succinylase; *dapE*, succinyl-diaminopimelate desuccinylase; *dapF*, diaminopimelate epimerase; *dapH*, tetrahydrodipicolinate acetylase; *dapL*, LL-diaminopimelate aminotransferase; *ddh*, diaminopimelate dehydrogenase; *lysA*, LL-diaminopimelate decarboxylase; *lysC*, aspartate kinase; *metA*, homoserine *O*-succinyltransferase/*O*-acetyltransferase; *metB*, cystathionine gamma-synthase; *metC*, cystathionine beta-lyase; *metH*, 5-methyltetrahydrofolate–homocysteine methyltransferase; *metK*, *S*-adenosylmethionine synthase; *metX*, homoserine *O*-acetyltransferase; *metY*, *O*-acetylhomoserine aminocarboxypropyltransferase; *metZ*, *O*-succinylhomoserine sulfhydrylase; *nifS*, cysteine desulfurase; *patA*, *N*-acetyl-LL-diaminopimelate aminotransferase; *ykuR*, *N*-acetyl- LL-diaminopimelate deacetylase.

File S1. KEGG maps showing detailed results on the pathways for the biosynthesis of amino acids in RmG30.

Table S1. GTDB-tk classification of strain RmG30 and other members of termite cluster I (shown in blue).

Table S2. Annotation details of the genes encoding metabolic pathways of strain RmG30 (Fig. 7). The genes are sorted by functional groups (in blue) and subgroups (in grey). Genes without gene ID were not found in the genome.